Structural Identification of a Novel Degradant of the Antibiotic Pirlimycin Formed Under Thermal Stress Conditions

Frank W. Crow [a], James R. Blinn [d] , Constance G. Chidestere [e], Anne M. Cooper [b], Wayne K. Duholke [a], John W. Hallberg [c], Gary E. Martin*[a], Richard F. Smith [a], and Thomas J. Thamann [a]

Pharmacia & Upjohn, Pharmaceutical Development, Kalamazoo, MI 49001-0199

Received September 17, 1999

The structure of a novel, thermally-induced degradant of the antibiotic pirlimycin is presented. The degradant was discovered during thermal stress stability testing of pirlimycin. The structure was determined using high resolution mass spectrometry, ms/ms fragmentation, and extensive nmr studies including a combination of homonuclear TOCSY and gradient, inverse-detected 2-D nmr experiments which included GHSQC and GHMBC. All nmr, high resolution ms and ms/ms fragmentation data are consistent with loss of a molecule of HCl during a ring closure involving one of the hydroxyl moieties from the sugar portion of the molecule forming a tetrahydrofurano[3,2-*b*]perhydropyran ring structure. The X-ray crystal structure is reported for pirlimycin. Using this structure molecular modelling studies are performed which demonstrate the feasibility of the formation of the new structure.

J. Heterocyclic Chem., **36**, 1049 (1999).

Introduction.

Pirlimycin (**1**) is a semi-synthetic lincosaminide antibiotic derived from lincomycin and approved for the treatment of clinical and subclinical mastitis in lactating dairy cattle. Pirlimycin (**1**), currently marketed as PIRSUE Aqueous Gel® (pathogen free), has demonstrated efficacy against mastitis-causing organisms including various *Staphylococcus (S. aureus)* and *Streptococcus (S. agalactiae, S dysgalactiae,* and *S. uberis)* species [1]. The mechanism of action of Pirlimycin (**1**) has been shown to occur through binding of the drug to the 50s ribosomal subunit of the bacterial ribonucleic acid, thus interfering with protein biosynthesis in the bacterium [2].

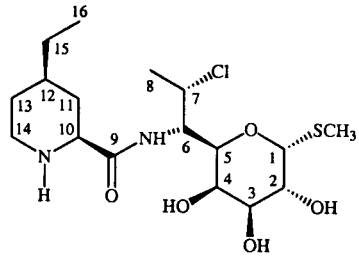

1

A sterile solution formulation of pirlimycin hydrochloride is currently under development. During routine registration stability studies, three batches of pirlimycin HCl sterile solution were subjected to thermal stress at 40° for four months. Storage under these conditions led to the formation of a previously unidentified degradation product at hplc rrt = 0.26 (relative to the pirlimycin) at a level of 0.2% of total peak area. This degradant was isolated, purified by preparative chromatography, and characterized using a combination of mass spectrometry and nmr spectroscopy.

Results and Discussion.

Characterization of Pirlimycin (**1**).

The structural identification of the impurity formed under thermal stress conditions relied heavily on comparisons to the mass spectral fragmentation and nmr resonance assignments and long-range heteronuclear correlation pathways of the parent molecule. Thus, despite the ^{1}H and ^{13}C chemical shift assignments that have been reported for pirlimycin (**1**), it is germane to briefly discuss the parent molecule first [3].

The nmr resonance assignments for pirlimycin and its degradant were begun from the three readily identified methyl resonances which include the thio-methyl, the 16-methyl of the ethyl side chain, and the 8-methyl group on the side chain adjacent to the sugar ring. These resonances were readily and unequivocally assignable on the basis of chemical shift, integration, and multiplicity. The thio-methyl group resonates as a singlet and, unfortunately, does not provide an entry point for further assignments that rely on homonuclear coupling pathways. In contrast, the 8-methyl doublet resonating at 1.34 ppm provides a starting point for the assignment of the proton resonances of the sugar portion of the antibiotic. Using successive connectivities contained in a homonuclear TOCSY spectrum, the side chain 7- and 6-methine proton resonances were assigned at 4.50 and 4.40 ppm, respectively. Sugar ring resonances were assigned in a similar fashion, including the hydroxyl protons. These assignments are presented in Table 1. The 16-methyl triplet arising from the ethyl side-chain in the piperidine-derived portion of the molecule provided a point of entry to the assignments in that subunit. The piperidine NH and amide NH resonances were assigned as the broad resonance at 8.90 and the doublet resonating at 8.40 ppm, respectively, the latter coupled to the H6 methine resonance. It is assumed that the piperidine NH resonance is shifted downfield as a result

Table 1

Proton and Carbon Chemical Shift Assignments for Pirlimycin (**1**) and Impurity **6** Recorded in Perdeuterodimethyl Sulfoxide.

Position	Pirlimycin (**1**) ^1H	Pirlimycin (**1**) ^{13}C	Cyclic Impurity **6** ^1H	Cyclic Impurity **6** ^{13}C
1	5.20	88.0	5.18 [1]	86.8
2	3.90	67.5	3.84	68.0
2-OH	5.09	-	5.18 [1]	-
3	3.37	70.2	3.59	68.1
3-OH	4.73	-	4.82	
4	3.77	67.4	4.24	78.3
4-OH	4.30	-	-	-
5	4.07	69.1	4.22	71.2
6	4.40	52.3	4.18	57.8
7	4.50	59.4	3.91	75.7
8	1.34	22.7	1.14	19.3
9 (C=O)	-	169.0	-	169.5
9-NH	8.40	-	8.33	-
10	3.77	57.3	3.67	57.4
10-NH	8.90 br	-	8.42 br	-
11'a, 11'b	1.20, 2.13	33.3	1.07, 2.13	33.4
12'	1.49	35.2	1.42	35.3
15'A	1.26	28.3	1.22	28.3
16'B	0.88	10.8	0.85	10.8
13'a, 13'b	1.17, 1.76	27.5	1.19, 1.71	27.8
14'a, 14'b	2.87,3.23	43.0	2.87, 3.18	43.2
1-SCH_3	2.04	12.3	1.98	12.1

br = broad peak. [1] integrates to 2 protons; GHSQC correlation to position #1 only.

of intramolecular interactions with the amide carbonyl and broadened through exchange.

Following the assignment of the proton nmr spectrum of **1**, the assignment of the protonated carbons followed directly from the GHSQC spectrum. At this point, there remained to be assigned only the amide carbonyl resonance whose assignment at 169.0 ppm was confirmed by long-range correlations to the H6 methine, the amide NH resonance, the H10 methine, and one of the H11 methylene resonances observed in a GHMBC spectrum. Correlations from the GHMBC spectrum also served to provide secondary confirmation of the proton assignments made from the homonuclear TOCSY spectrum. Rather than discussing the long-range correlations observed for pirlimycin (**1**), the connectivities are summarized in Scheme 1.

Scheme 1

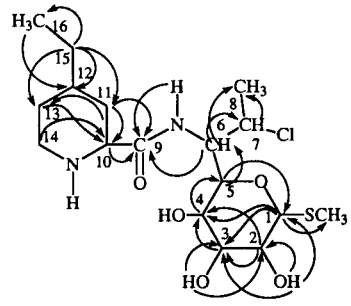

The ms analysis using FAB (fast atom bombardment) produced a protonated molecular ion for pirlimycin, MH^+ = 411 amu. The ms/ms fragmentation of the protonated molecular ion resulted in fragmentation (see Scheme 2) wholly consistent with the structure of pirlimycin (**1**).

Most of the fragmentation is dominated by sequential losses of the neutral molecules of either H_2O or CH_3SH which generate unsaturated sites in the sugar ring. There are also a number of significant skeletal fragmentations. The ion at m/z = 112^+ corresponds to the 4'-ethyl-2'-piperidine ring while the ion at m/z = 272 is the result of loss of the 4'-ethyl-2'-piperidine ring with charge retention, this time, on the sugar side of the molecule. The ion at m/z = 321 is the result of an internal fragmentation of the sugar ring.

Structural Characterization of the Thermal Stress Degradant.

Following the observation of a previously unidentified degradant by analytical hplc methods, mass analysis was undertaken using ESI lc/ms. The degradant peak gave a protonated molecular ion at m/z = 375 amu. The mass difference relative to the parent drug was 36 amu, suggesting a loss of HCl from pirlimycin, further supported by the pronounced absence of the ^{37}Cl isotope peak normally seen with pirlimycin. The loss of HCl was confirmed, after preparative isolation, using high resolution mass spectrometry. The accurate mass was measured as 374.18759

Scheme 2

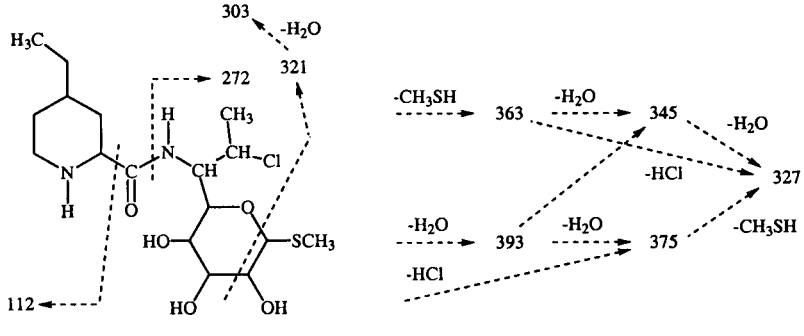

amu, which fits to within 0.11 ppm of a theoretical molecular weight for a molecule with the formula $C_{17}H_{30}N_2O_5S$.

Confirmation that the impurity was a dehydrohalogenation product, presumably derived from pirlimycin, raises the question of where HCl was lost from the molecular framework and what is the corresponding structure of the degradant. Several possible pathways are available for the loss of HCl, which are summarized by Scheme 3.

Scheme 3

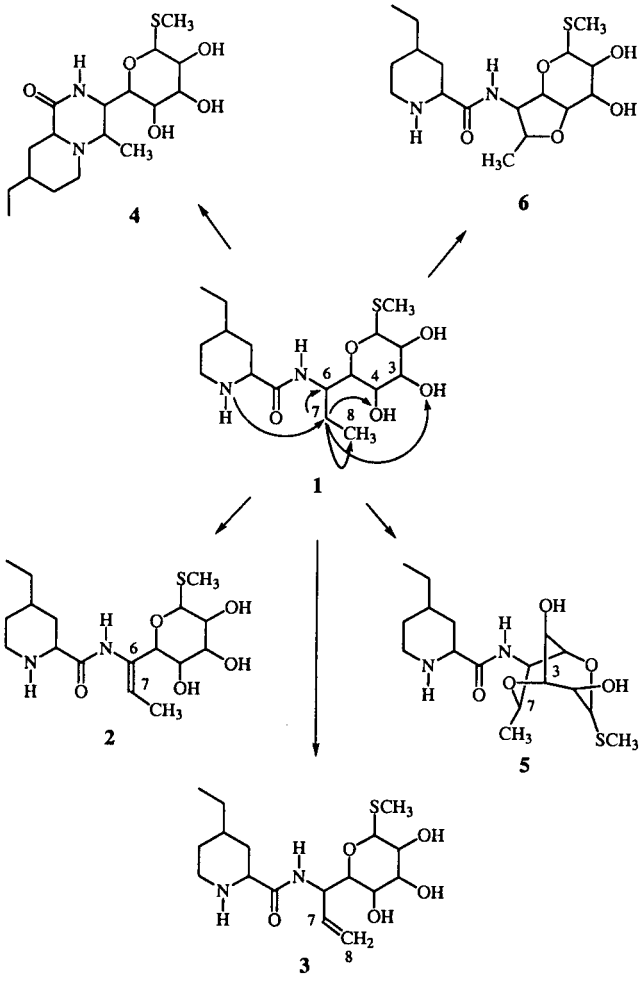

Two possible routes involve the loss of HCl entirely within the chloroethyl sidechain adjacent to the sugar portion of the molecule leading to the corresponding vinylic structures **2**, and **3**. Another possibility involes the loss of hydrogen from the NH of the piperidine portion in an intramolecular cyclization giving rise to the corresponding piperidinopiperazine-containing molecule, **4**. Plausible losses of hydroxyl protons from the 3-OH to give the corresponding tetrahydropyranyl ring joined to the sugar, **5**, or from the 4-OH to give a tetrahydrofuranyl ring joined to the sugar ring, **6**, must also be considered.

Having considered the possible routes leading to the loss of HCl the nmr data for the degradant are compared to that of pirlimycin (**1**). Proton and carbon resonance positions for the (4'-ethyl-2'-piperidinyl) carbonyl moiety of the molecule are virtually unchanged, essentially ruling out the formation of the piperidinopiperazine-containing species, **4**. The ms/ms collisional activation of pirlimycin and the degradant produced an intense fragment ion at m/z = 112 amu for both molecules, see Scheme 1. This ion corresponds to the intact 4'-ethyl-2'-piperidine frament ion corroborating that the piperidine ring is unchanged in the degradant, thereby eliminating **4** from consideration as a possible structure of the degradant.

Examination of the ^{13}C nmr spectrum of the degradant readily allows the elimination of **2** and **3** from consideration; there were no vinyl carbon resonances in the spectrum, which would be required if either of these structures were involved. Thus, based on a very cursory examination of the mass spectral data and carbon nmr spectrum, the problem has been reduced to differentiating between structures **5** and **6**.

Scheme 4 shows the ms/ms fragmentation obtained from collisional activation of the protonated molecular ion for the impurity, m/z = 375$^+$. As in pirlimycin, the fragmentation is mostly the result of losses of H_2O and CH_3SH molecules from the sugar portion of the molecule. Ring fragmentation also takes place, but does not allow differentiation between structures **5** and **6**.

Scheme 4

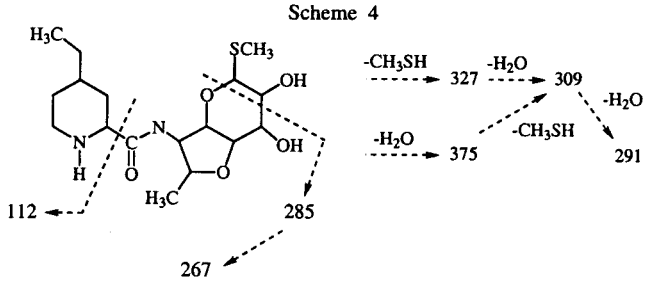

Establishing the structure of the thermal stress degradation product of pirlimycin (**1**) requires the unequivocal assignment of the proton and carbon resonances in the sugar portion of the molecule and an examination of the long-range correlations exhibited by these resonances in the GHMBC spectrum. Thus, in a fashion analogous to that described above for the parent molecule, the 8-methyl doublet was used as a point of entry into the assignment of the sugar of the molecule *via* a homonuclear TOCSY spectrum. Once again, protonated carbon resonance assignments followed directly from the GHSQC spectrum of the degradant.

With the proton resonances sequenced and the proton-carbon resonant pairings in hand, it is reasonable to begin to make comparisons to the assigned spectra of the parent molecule. Thus, the proton/carbon chemical shifts for the resonance pairings at the 1-, 2-, and 3-positions of

the degradant were in reasonable correspondence with those of the corresponding positions of the parent molecule. In contrast, H4 was shifted downfield by nearly 0.5 ppm while C4 was shifted downfield from 67.4 to 78.3 ppm. The 5-position chemical shift assignments, again, were in reasonable agreement with those of the parent drug. Likewise, the H7/C7 resonant positions shifted from 4.50/59.4 ppm to 3.91/75.7 ppm in the degradant, consistent with the displacement of the 7-chloro substituent by an oxygen. These data strongly suggested that the proton loss had come from the 4-OH group leading to the formation of a tetrahydrofurano-perhydropyran bicyclic moiety in the degradant as shown by **6**.

Long-range correlations in the GHMBC spectrum were finally used to confirm the structure of the degradant as **6**. In particular, the H4 methine proton resonating at 4.24 ppm was long-range coupled *via* three-bonds through the ether linkage [4] to the C7 resonance at 75.7 ppm. The complementary long-range coupling from H7 to C4 was also observed, but was substantially weaker than that from H4 to C7. Other long-range correlations observed for the tetrahydrofurano-perhydropyran moiety are shown in Scheme 5.

Scheme 5

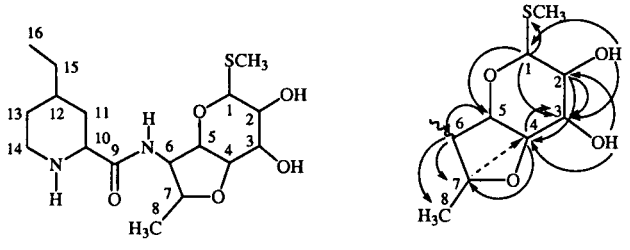

X-Ray Structure And Molecular Modelling of Pirlimycin.

Molecular modelling was employed to determine if the reaction to produce structure **6** was feasible and if it were the most logical from an energetic standpoint. The X-ray structure for pirlimycin was solved by direct methods, using DIREC [5]. Hydrogens were found in a difference Fourier map after a few cycles of refinement; final least squares refinement included coordinates for all atoms and anisotropic thermal parameters for nonhydrogen atoms. The function minimized in the refinement was $\Sigma W(Fo^2 - Fc^2)^2$, where weights w were $1/\sigma^2 (Fo^2)$. The absolute configuration of several centers was known prior to the x-ray structure determination. Anomalous dispersion factors [6] were included in the final refinement cycles. In the final cycle all shifts were $<0.2\sigma$. The final agreement index R was 0.033 for all 2161 reflections, and 0.030 for the 2008 reflections having $Fo^2>3\sigma$. The standard deviation of fit was 1.9. Atomic form factors were from Doyle and Turner [7], and, for hydrogen, from Stewart, Davidson, and Simpson [8]. The CRYM system of computer programs [5] was used for structure refinement.

Figure 1 shows the hydrogen bond between the amide nitrogen and the ethanol oxygen; the nitrogen is the donor in this case. The hydrogen attached to the ethanol oxygen participates in a hydrogen bond with the chlorine ion. The sugar hydroxyl at 4 also forms a hydrogen bond to the chlorine ion, but this is not shown in the figure because the bond is with the ion related by 2_1 symmetry. The piperidine nitrogen is protonated; one hydrogen forms a bifurcated hydrogen bond to the other two sugar hydroxyls (O2 and O3) in a molecule also related by the 2_1 axis, but translated by 1 in y; the other hydrogen on the piperidine nitrogen has a close approach to the chlorine ion, 2.43 Å, but the nitrogen-to-chlorine distance is rather long for an interaction, 3.293 Å.

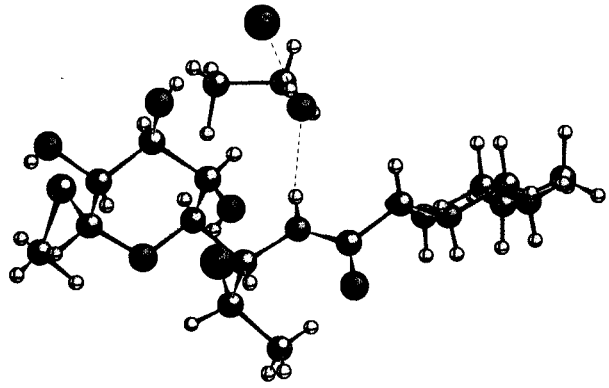

Figure 1. X-ray Crystallographic Structure of Pirlimycin HCl Ethanol Solvate.

Starting from the above crystal structure, conformational searching of protonated pirlimycin in water was used to look for conformers which were set up properly for internal cyclization to structures **4, 5,** and **6**, and to assess their energetic accessibility. The search yielded a total of 561 unique conformers within 7.5 kcal/mole of the global minimum. These structures were geometrically filtered for conformers which were properly set up for the various possible internal cyclizations. Despite finding 47 *cis*-amide conformers, the lowest-energy of which was 3.0 kcal/mole above the global minimum, no conformers were found which placed the piperidine nitrogen within even 4.5 Å of C7; cyclization to **4** is thus unlikely. Similarly, no conformations were found which placed O3 within 4.5 Å of C7, rendering unlikely the formation of **5**. In contrast, 42 geometrically-appropriate conformers for cyclization to **6** were found, the lowest-energy of which was 3.5 kcal/mole above the global minimum (Figure 2). These conformers all placed O4 and C7 in close contact (O4-C7 distances of 2.94-3.02 Å) and had a

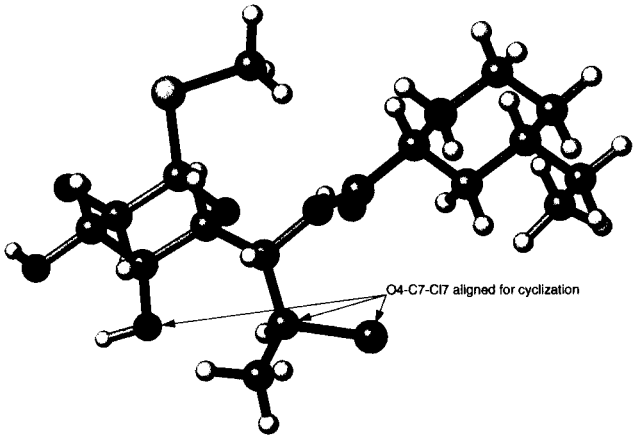

Figure 2. Lowest-energy Pirlimycin Conformer Appropriate for Cyclization.

near-collinear arrangement of O4, C7, and C17 (O4-C7-Cl7 angles of 158-165°), and are thus favorable for cyclization to **6** *via* S_N2 displacement of Cl7 by O4. A model of **6** is shown in Figure 3.

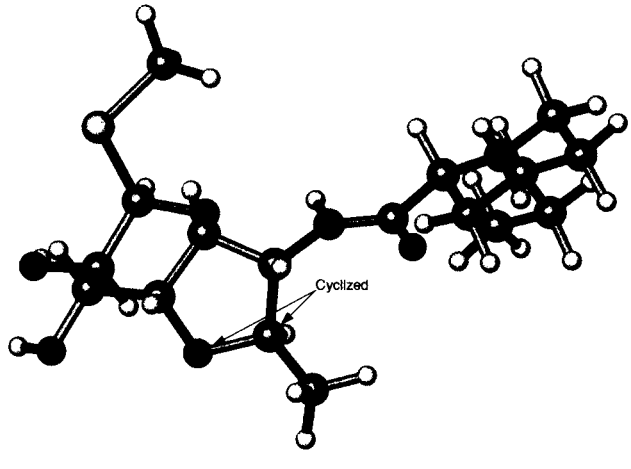

Figure 3. AMBER*-minimized Model of the Cyclization Product **6**.

Conclusion.

A previously unidentified degradation product of pirlimycin (**1**) is reported, resulting from cyclization of pirlimycin with loss of HCl. Characterization by ms and nmr demonstrated the product to be the bicyclic perhydrofurano[3,2-*b*]pyran (**6**), resulting from attack of the C4 hydroxyl on C7. Starting from the X-ray structure of pirlimycin, molecular modeling confirmed that in contrast to other possible ring-closures, cyclization to **6** *via* an S_N2 mechanism is quite feasible.

Table 2

Fractional Coordinates (x 10^4) and Beq for Pirlimycin Standard Deviations are in Parentheses.

$Beq = 4/3(a^2B_{11}+b^2B_{22}+c^2B_{33}+abcosyB_{12}+accos\beta B_{13}+bccos\alpha B_{23})$

	x	y	z	Beq (Å2)
CL	12202 (1)	5640 (1)	6339(1)	1.79(3)
CL7	7614(l)	1901	8927(1)	2.29(4)
S	11359(1)	18(2)	7578(1)	1.79(3)
O1	8839(2)	715 (3)	6469(2)	1.14(9)
C1	10248(3)	136(4)	6370(2)	1.25(13)
C1M	10277(6)	-1158(7)	8172(4)	3.81(24)
C2	11077(3)	869(4)	5575(2)	1.24(14)
O2	12526(3)	382 (3)	5477(2)	1.59(11)
C3	11198(4)	2278(4)	5847(2)	1.24(14)
O3	11952(3)	2911(3)	5088(2)	1.70(11)
C4	9657(4)	2839(4)	5971(2)	1.15(14)
O4	8744 (3)	2945(3)	5052(2)	1.29(10)
C5	8934(3)	2038(4)	6771(2)	0.91(13)
C6	7350(3)	2447(4)	6898(2)	1.03(13)
N6	7312(3)	3806(3)	7090(2)	1-09(12)
C7	6606(4)	1671(5)	7699(3)	1.46(15)
C8M	4997(4)	2026(5)	7766(3)	1.85(16)
C9	6349(3)	4580(4)	6555(2)	1.02(13)
O9	5398(3)	4205(3)	5920(2)	1.37(10)
C10	6476(3)	5973(4)	6853(2)	1.15(14)
C11	5855(4)	6192(4)	7892(3)	1.26(14)
C12	5677(4)	7587(4)	8165(2)	1.28(14)
C13	4777(4)	8265(5)	7308(3)	1.22(14)
N14	5594(3)	6727(4)	6052(2)	1.17(11)
C14	S475(4)	8123(4)	6312(2)	1.35(14)
C15	4983(5)	7693(5)	9183(3)	2.03(17)
C16	4706(5)	9058(5)	9533(3)	2.37(19)
C2ET	11418(7)	3968(8)	9080(5)	4.65(28)
OET	9805(3)	5278(4)	7931(2)	2.47(12)
C1ET	10553(5)	5196(6)	8920(4)	3.33(21)

EXPERIMENTAL

Isolation and Preparation.

A pirlimycin degradation product with a relative retention time of 0.26 was isolated from a sample of sterile solution pirlimycin 50 mg/ml which had been stressed at 70°. The degradant was present in this stressed solution at 4.2% of the total peak area. Gradient semi-preparative hplc chromatography using a 20 x 250 mm, Kromasil C-8, 10 micron column and a 3 solvent system was used for the isolation. The mobile phase gradient for first stage purification ran from 3% 2-propanol in 0.1 *M* ammonium phosphate, monobasic buffer to 25% 2-propanol in monobasic ammonium phosphate buffer over 30 minutes. This was used to isolate the impurity. The second stage was an 8% methanol in water mobile phase used to wash the remainder of the material off of the column. About 2 ml of pirlimycin HCl sterile solution was diluted with 3 ml of 3% mobile phase and 5 ml of this solution was injected. A variable wavelength uv detector set at 214 nm was used for peak detection. Fractions of the impurity were collected, pooled, and roto-evaporated to dryness at 42°/70 mbar. The impurity was extracted from the ammonium phosphate with acetonitrile. The acetonitrile was removed by lyophilization. The impurity isolate was determined to be approximately 85% pure by analytical hplc.

Table 3

Bond Lengths (Å) and Angles (°) for Pirlimycin.

CL7	C7	1.814 (4)	C7	C8m	1.512 (5)		
S	C1	1.824 (3)	N6	C9	1.348 (5)		
S	C1M	1.790(6)	C9	O9	1.219(4)		
O1	C1	1.427(4)	C9	C10	1.508(6)		
O1	C5	1.439(5)	C10	N14	1.498(5)		
C1	C2	1.541(5)	C10	C11	1.540(5)		
C2	O2	1.422 (4)	N14	C14	1.503 (6)		
C2	C3	1.517(6)	C13	C14	1.511(5)		
C3	O3	1.420(5)	C12	C13	1.518(5)		
C3	C4	1.534 (5)	C12	C15	1.533 (5)		
C4	O4	1.419(4)	C11	C12	1.512 (6)		
C4	C5	1.533 (5)	C15	C16	1.525(7)		
C5	C6	1.518(4)	C2ET	C1ET	1.508(10)		
C6	C7	1.530(5)	OET	C1ET	1.427(5)		
C6	N6	1.442(5)					
C1	S	C1M	98.5(2)	CL7	C7	C6	109.4 (2)
C1	O1	C5	113.4 (3)	CL7	C7	C8M	109.6 (3)
S	C1	O1	112.6(2)	C6	C7	C8M	112.9(3)
S	C1	C2	111.5(2)	C6	N6	C9	121.4(3)
O1	C1	C2	109.8(3)	N6	C9	O9	124.2(4)
C1	C2	O2	112.8(3)	N6	C9	C10	114.1(3)
C1	C2	C3	110.5(3)	O9	C9	C10	121.6(3)
O2	C2	C3	108.5(3)	C9	C10	N14	107.2(3)
C2	C3	O3	108.3(3)	C9	C10	C11	110.5(3)
C2	C3	C4	110.2(3)	C11	C10	N14	109.9(3)
O3	C3	C4	112.9(3)	C10	N14	C14	113.0(3)
C3	C4	O4	114.3(3)	C13	C14	N14	109.7(3)
C3	C4	C5	107.9(3)	C12	C13	C14	111.6(3)
O4	C4	C5	112.5(3)	C13	C12	C15	112.9(3)
O1	C5	C4	110.5(3)	C11	C12	C13	109.3(3)
O1	C5	C6	105.3(3)	C11	C12	C15	109.8(3)
C4	C5	C6	112.4(3)	C12	C15	C16	115.0(4)
C5	C6	C7	113.5(3)	C10	C11	C12	114.2(3)
CS	C6	N6	109.4(3)	C2ET	C1ET	OET	112.6(5)
C7	C6	N6	112.3(3)				

Table 4

Hydrogen Bonds for Pirlimycin. D Represents Donor, A Acceptor; Distances are in Å and Angles are in °. Standard Deviations are in Parentheses

D	A	A	AT	D...A	H...A	<,D-H ...A
OET	CL	x, y,	z	3.161(3)	2.46(4)	172(9)
N6	OET	x, y,	z	2.881(4)	2.07(4)	164(10)
O2	O4	2-x, y-1/2,	1-z	2.856(4)	2.34(5)	160(11)
N14	O2	2-x, y+1/2,	1-z	3.081(4)	2.45(4)	139(9)
N14	O3	2-x, y+1/2,	1-z	3.043(4)	2.47(4)	131(10)
O4	CL	2-x, y+1/2,	1-z	3.108(3)	2.43(4)	169(9)

NMR Spectroscopy.

The nmr spectra were acquired using samples of pirlimycin and the impurity that were dissolved in perdeuterodimethylsulfoxide. A Bruker AMX-400 operating at 400.13 MHz for ^1H observation, was used for 1D ^1H and all 2D experiments. A Bruker AMX-500 operating at 125.77 MHz was used for ^{13}C experiments. Proton and carbon spectra were assigned using a number of 2D nmr experiments. Homonuclear TOCSY [9] with mixing times of 19, 39, and 80 msec. were used to establish proton-proton connectivities. GHSQC [10] was employed to establish direct or one-bond ($^1J_{CH}$) proton-carbon heteronuclear correlations, and GHMBC [11] optimized at 7.8 Hz was used to establish long-range proton-carbon coupling pathways.

Mass Spectrometry.

Low resolution full scan mass spectra and ms/ms spectra were acquired on a Finnigan TSQ-700 Triple Sector Quadrupole mass spectrometer using ESI (electrospray ionization) for the lc/ms analysis and FAB (fast atom bombardment) ionization with thioglycerol as a FAB matrix for analysis of the purified sample. Sample isolates were dissolved in acetonitrile or methanol and one microliter of this solution was added to one microliter of thioglycerol. Full scan data were recorded in the "Q3" mode at unit mass resolution. MS/MS data were acquired in the "daughter" mode, selecting the protonated molecular ion in Q1 and collisionally activating it at *ca.* 10-20 eV in Q2 and scanning the fragments in Q3.

High resolution accurate mass measurement was performed on a Kratos MS-50 double focusing mass spectrometer operating at a resolution of 10,000 (10% valley). LSIMS (liquid secondary ion MS) ionization was used with glycerol as a sample matrix. The accurate mass was measured versus glycerol adducts.

X-ray Structure Determination.

Pirlimycin $C_{17}H_{32}N_2O_5SCl^{(+)}\cdot Cl^{(-)}\cdot C_2H_5OH$; formula wt. = 410.97•36.46•46.07; monoclinic; space group $P2_1$; Z=2; a = 9.052(1), b = 10.438(1), c = 13.220(1)Å, β = 94.42(1)°, V =1245.2(2) Å^3; calculated density = 1.31 g cm^{-3}; absorption coefficient μ = 3.28 mm^{-1}; clear plate 0.04 x 0.16 x 0.36 mm mounted on a glass fiber. Intensity data were measured at low temperature, -120°, on a Siemens P1bar diffractometer using graphite monochromatized Cu Kα radiation, (λ(CuKα) = 1.5418Å), with 2θ max = 135°. θ/2θ step scans were used with scan widths ≥3.4° and a scan rate of 1°/minute; 2161 unique reflections. Ten reflections periodically monitored showed no trend towards deterioration; σ^2(I) was approximated by σ^2(I) from counting statistics + (dI)^2, where the coefficient of I was calculated from the variations in intensities of the monitored reflections and was 0.02. Cell parameters were determined by least squares fit of K$\alpha_1$2θ values (λ(Kα_1) = 1.5402) for 25 high 2θ reflections [12]. An Lp correction appropriate for a monochromator with 50% perfect character was applied, and the data were corrected for absorption [13]. X-ray coordinates and equivalent isotropic thermal parameters are listed in Table 2, bond distances and angles in Table 3 and hydrogen bond parameters in Table 4. Structural parameters have also been deposited in the Cambridge Structural Database.

Molecular Modeling.

Molecular modeling was performed using the Mosaic-2 modeling package [14]. Energy calculations used BatchMin 4.5 [15]; the SUMM (systematic unbounded multiple minimum) method [16] was used for conformational searching. The search was 20,000 steps, use-directed, with a 7.5 kcal/mole energy window; all nontrivial torsions were varied, including the rings, hydroxyls, and amide. The AMBER* forcefield [17] was used, with the GB/SA water solvation model [18] and extended nonbonded cutoffs; no low-quality torsional parameters were required. The initial pirlimycin structure for conformational searching was taken from the crystal structure, and was modeled in the protonated state. A total of 561 conformers were found within 7.5 kcal/mole of the global minimum; no new conformers were found during the last 1000 steps of the search, which can thus be taken to be

adequately converged. The conformational searching results were filtered for structures possessing an appropriate geometry for various potential cyclizations. There were no conformers in which the piperidine nitrogen, O3, O2, or S1 approached within 4.5 Å of C7. However, 42 conformers were obtained which were appropriate for internal S_N2 ring closure to structure **6** (filter: O4-C7 distance ≤3.3 Å and O4-C7-Cl angle 180±40°; actual values were in the range 2.94-3.02 Å, 158-165°). The lowest-energy of these conformers was 3.5 kcal/mole above the global minimum. A highly approximate calculation (neglecting entropy) predicts that these conformers should constitute on the order of 0.1% of the total pirlimycin population at room temperature.

REFERENCES AND NOTES

* To whom inquiries should be addressed: Pharmacia & Upjohn, Pharmaceutical Development, Rapid Structure Characterization Group, MS# 4821-259-277, Kalamazoo, MI 49001-0199. [a] Rapid Structure Characterization Group - Pharmaceutical Development. [b] Pharmaceutical Development - Animal Health Products. [c] Clinical Development - Animal Health Products. [d] Computer-Aided Drug Discovery. [e] Structural, Analytical and Medicinal Chemistry.

[1] NADA 140-036, Treatment of Clinical and Subclinical Mastitis in Lactating Dairy Cattle.

[2] J. D. C. Jao and R. C. Moellering, Jr., "Antibacterial Agents," Manual of Clinical Microbiology, 6th ed, P. R. Murray, E. J. Baron, M. AmPfaller, F. C. Tenover and R. H. Yolken, eds, Am. Soc. Microbiol., Washington, DC, 1995, p 1281.

[3] V. P. Marchall, J. E. McGee, J. I. Cialdella, L. Baczynskyj, D. G. Chirby, D. A. Yurek, W. F. Liggett and M. S. Kuo, *J. Antibiot.*, **44**, 895 (1991).

[4] R. C. Crouch, G. E. Martin, R. W. Dickey, D. G. Baden, R. E. Gawley, K. S. Rein and E. P. Mazzola, *Tetrahedron*, **51**, 8409 (1995).

[5] D. J. Duchamp, DIREC, a direct methods program for solving structures, and CRYM, a system of crystallographic programs, (1984). Pharmacia & Upjohn, Kalamazoo, MI.

[6] D. T. Cromer and D. Liberman, *J. Chem. Phys.* **53**,1891 (1970).

[7] P. A. Doyle and P. S. Turner, *Acta Crystallogr.*, **A24**, 390 (1968).

[8] R. F. Stewart, E. R. Davidson and W. T. Simpson, *J. Chem. Phys.*, **42**, 3175 (1965).

[9] L. Braunschweiler and R. R. Ernst, *J. Magn. Reson.*, **53**, 521 (1983).

[10] G. Bodenhausen and D. J. Ruben, *Chem. Phys. Letters*, **69**, 185 (1980); a gradient-enhanced version of this experiment is now in use in these laboratories - G. S. Walker, P. E. Fagerness, K. A. Farley, and S. A. Mizak, *J. Heterocyclic Chem.*, **34**, 295 (1997).

[11] A. Bax and M. F. Summers, *J. Am. Chem. Soc.*, **108**, 2093 (1986). The gradient-enhanced version now in use is that described by: R. E. Hurd and B. K. John, *J. Magn. Reson.*, **91**, 648 (1991).

[12] D. J. Duchamp, *ACS Symp. Ser.* , **46**, 98 (1977).

[13] W. R. Busing and H. A Levy, *Acta Crystallogr.*, **10**, 180 (1957).

[14] J. B. Moon, J. R. Blinn, M. W. Schulz, Pharmacia & Upjohn, unpublished.

[15] F. Mohamadi, N. G. J. Richards, W. C. Guida, R. Liskamp, C. Caufield, G. Chang, T. Hendrickson, and W. C. Still, *J. Comput. Chem.*, **11**, 440 (1990).

[16] J. M. Goodman and W. C. Still, *J. Comput. Chem.*, **12**, 1110 (1991).

[17] S. J. Weiner, P. A. Kollman, D. T. Nguyen, and D.A. Case, *J. Comput. Chem.*, **7**, 230 (1986); Ferguson, D. M.; Kollman, P. A. *J. Comput. Chem.*, **12**, 620 (1991).

[18] W. C. Still, A. Tempczyk, R. C. Hawley, and T. Hendrickson, *J. Am. Chem. Soc.*, **112**, 6127 (1990).